Geosynthetics, J. Kuwano & J. Koseki (eds)
© 2006 Millpress, Rotterdam, ISBN 90 5966 044 7

# Investigation of the behaviour of geosynthetic/soil systems in reinforced-soil structures

Aschauer, F. & Wu, W.
*Institute of Geotech. Eng, University of Natural Resources and Applied Life Sciences, Austria*

Oberreiter, K.
*Polyfelt Ltd., Austria*

Keywords: geogrid-reinforced structure, extensometer evaluation, critical failure surface, creep behaviour

ABSTRACT: In this paper, a full-scale test on geosynthetics reinforced slope (13 m high and 26 geogrid layers) is reported. The mechanical properties of the fill material and the reinforcement are investigated in laboratory. The testing slope is extensively instrumented by multiple extensometers, horizontal inclinometers and geodetic survey. The test data are presented and discussed. Some implications for the design of geosynthetics reinforced slopes are given.

## 1 INTRODUCTION

Geosynthetic reinforced slopes often provide a time saving and cost effective alternative to the conventional earth retaining structures. Geogrids were first used to reinforce soil slopes in Europe in 1980. It is now commonly used to reinforce and steepen new embankment slopes for roadways, parking areas and commercial building sites. The interaction between soil and geogrids and the longterm performance is rather complex and not yet fully understood. Recently, much progress has been made to gain insights into the mechanism of the interaction between soil and geogrids.

However, there is very little experimental work on geogrid reinforced slopes in the literature. In particular, large scale tests on geogrid reinforced slopes are extremely scarce. Model tests on geogrid reinforced slope with a height of 3 m were recently reported by Bathurst et al. (2003). Well defined and extensively instrumented large scale tests provide invaluable data base to improve the design methods based on the limit state equilibrium and to verify the more sophisticated design methods, e.g. finite element method, using advanced constitutive models for the fill materials.

The present paper reports a large scale test on a geogrid reinforced steep slope. The 13 m high and 70° steep slope (Figure 1) has been extensively instrumented. The mechanical properties of the fill material and the geogrid are investigated and well documented. After the test slope was completed in 1996, the geotechnical instrumentation has been continued until now to study the longterm performance of the geogrid reinforced slope.

Figure 1. Testing slope with geogrid reinforcement.

## 2 PRELIMINARY DESIGN

The design is based on ÖNORM (1999) under consideration of internal and external stability analysis using limit equilibrium method. The calculation is based on partial safety factors. The safety factor for the friction angle of fill material is 1.3. The safety factor for the geogrid is 1.0.

The external stability is examined by conventional methods with the reinforced structure regarded as a monolithic body. The design of the internal stability is carried out using the method of local mobilisation (Shaigani et al. 2005). This method is based on the slice method of limit equilibrium taking into account of the different levels of strength mobilisation of fill material and reinforcements. For the chosen geogrid ($t_1$ = 45 kN/m), an anchor length of 8.0 m is obtained. In order to optimise the design, the reduced anchor length of 6.5 m is used.

## 3 CONSTRUCTION DETAILS

The fill material consists of well graded construction debris. In order to achieve optimal compaction, large boulders are sorted out. Furthermore, the mass passing through the sieve with the mesh size of 0.06 mm shall be within the range 15% < $D_{0.06}$ < 40%. The fill material (50 cm thick) is placed and compacted with a single drum vibratory roller. The zones along the borders are compacted manually with a tamper. Afterwards, the geogrid matt is wrapped over the compacted fill with an embedment of 6.5 m. The geogrid matt for the next layer is placed to give an overlapping of 1.5 m. After the slope construction is completed, the slope surface is protected with a 2 cm thick concrete cover.

The density and water content after compaction is controlled in place by the conventional sand replacement and nuclear gauge. In addition, pocket penetrometer tests and loading plate tests are carried out. The mean water content is about 9.8%. The density varies between 18.4 and 21.3 kN/m$^3$. The deformation modulus from loading plate ranges from 3.5 to 18.6 MPa. The low values are obtained near the slope surface (poor compaction), while the high values are obtained in the rear part of the slope (good compaction).

The laboratory tests of the fill materials include grading tests, Proctor tests and direct shear tests. The specific gravity of the solid varies between 2.64 g/cm$^3$ and 2.71 g/cm$^3$. The Proctor density lies between 1.88 t/m$^3$ and 2.28 t/m$^3$. The friction angle shows very low scatter around the mean value of about 33.5°.

The testing slope is reinforced by high strength geogrid (PET yarns) with high stiffness, high friction and low creep. The mechanical properties of the geogrid with an average mass of 360 g/m$^2$ are provided by the manufacturer: $t_1$ = 45 kN/m, $t_2$ = 18 kN/m, $\varepsilon_1$ = 15%, $\varepsilon_2$ = 13%, where $t_1$ and $t_2$ are the tensile strength and $\varepsilon_1$ and $\varepsilon_2$ the corresponding strain along the two principal directions of geogrid. The design strength is assumed to be 21.6 kN/m.

## 4 GEOTECHNICAL INSTRUMENTATION

The testing slope is accompanied by an extensive geotechnical instrumentation programme, which comprises mainly of extensometers, horizontal inclinometers and also geodetic survey.

### 4.1 *Extensometer*

Three horizontal multiple extensometers (6 points) are installed to measure the extension of the geogrid and the horizontal deformation of the fill material. The three extensometers (A, B and C) are located at the level of 2.5 m, 5.5 m and 10.5 m above ground. Glass fibre rods are used instead of steel rods to minimize the effect of temperature. The geogrid is fixed to a steel plate located in the rear side of the slope. The steel plate serves as the anchor plate for the extensometer. The glass fibre rods are protected by glass fibre tubing to minimize the friction of the fill material. The extensometers are embedded in sand to avoid damage caused by the coarse fill material during compaction.

### 4.2 *Horizontal inclinometer*

The settlement is measured by three 9 m long horizontal inclinometers (1, 2 and 3) at the level of 3 m, 6 m and 10 m above ground. The inclinometer pipes with a length of 3 m are connected by water tight couplings. Like the extensometers, the horizontal inclinometers are also embedded in sand.

### 4.3 *Geodetic survey*

In addition, some geodetic survey is performed in order to measure the deformation of the slope surface. The survey points are placed at the centre of each layer between two adjacent geogrid sheets. Further survey points are set at the heads of the extensometer and horizontal inclinometer rods. The spatial coordinates are obtained via intersections from fixed points in a distance of about 10 m. In order to enhance the accuracy of the vertical measurements two additional fix points are placed in the rock ground beside the testing slope.

## 5 TEST RESULTS

Based on the measurements the displacement field for the cross section in the centre of the slope can be obtained with 129 exterior and interior measurement points. These measurements are described below.

### 5.1 *Extensometer*

Typical results of the extensometer B are shown in Figure 2. A simultaneous increase of strain along with the construction steps can be observed. A perusal of the data shows a steep rise of strain in the first one-third near the slope surface. Beyond the one-third the strain remains virtually unchanged. With increasing slope height, the maximum strain moves to the interior of the slope. This corresponds well with the fact that the potential slide surface shifts gradually to the interior with increasing slope height.

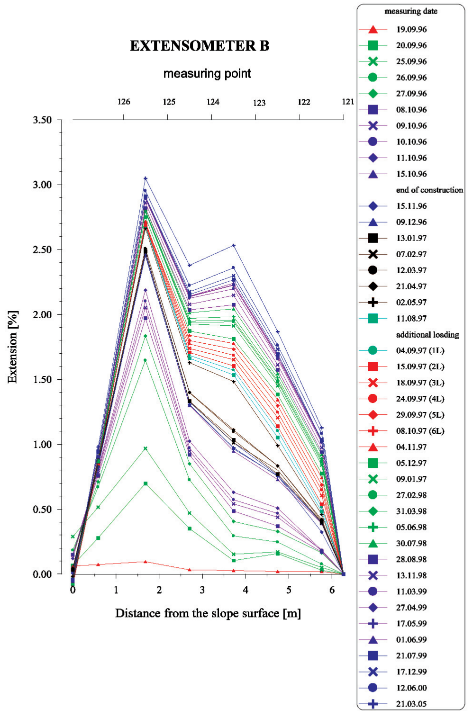


Figure 2. Data from extensometer B.

The maximum strain is about 3.5 % with reference to a length of 1 m, which lies well below the strain of tensile failure for the geogrid ($\varepsilon_1 = 15\%$).

In general, the maximal strains increase only slightly after construction completion. However, the strains in the rear part of the slope show larger increase than in the front part of the slope. This gives rise to a relatively uniform strain distribution in the horizontal direction. A steep decrease towards the slope surface and the end of the geogrid can be observed.

## 5.2 *Horizontal inclinometer*

The maximum settlement of e.g. the horizontal inclinometer 2 is about 40 cm near the slope surface and 25 cm in the rear part of the slope. The large settlement in the zone near the slope surface is ascribed to the deformation caused by the frost-thaw cycles in winter. Most part of the settlement is obtained during construction.

The vertical deformations are more pronounced in the less compacted fore part than in the rear part. It seems that the deformations are influenced by the initial settlements in the front part and by settlement due to consolidation of the fill material in the rear part of the slope.

## 5.3 *Geodetic survey*

During the first year after construction completion, large displacements in the front part are observed. They can be ascribed to initial settlements of the poorly compacted front part of the slope. Further influential factors are the wetting-drying after heavy rainfall and frost-thaw cycles in winter. Note that the slope surface was not covered by concrete in this period.

The deformation pattern can be described as follows. Frost induced heave up to 18 mm has been observed. Settlements are observed during construction. The maximum deformations are obtained during construction. After construction completion (October 1997), the settlement rate decreases. Until now, a maximum settlement of about 50 cm is registered at the height of 5.0 m, where the settlement after construction accounts to about 44 cm. The horizontal displacements (Y-direction) in the lower layers are comparatively small. This is because the first geogrid matt is embedded to the ground. The horizontal displacements increase with the height and reach their maxima at the half slope height. Beyond this slope height, the horizontal displacements show a decreasing tendency towards the slope crown.

## 5.4 *Displacement trajectories*

The overall displacement field is shown in Figure 3, where the results of the different measurements are compiled. The origins of the displacement trajectories are situated at the coordinates of the initial measurement. The trajectories are composed of the displacements measured on certain dates. By establishing a triangular mesh, the displacement at an arbitrary time can be obtained by interpolation and a direct comparison with the deformation of the finite element analysis is possible.

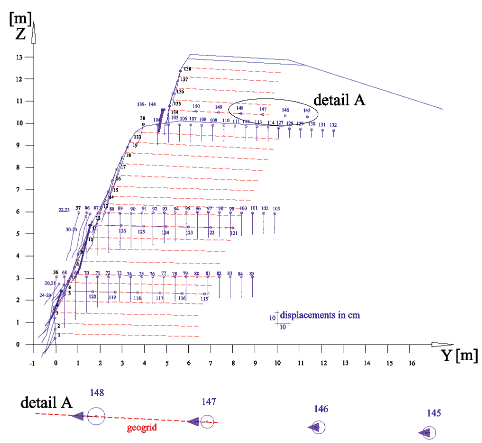


Figure 3. Displacement trajectories.

Considering extensometer C over the entire measurement period, the reinforced soil structure displaces away from the backfill like a monolith body. An analogous behaviour was also observed in a centrifuge test with the scale of 1:20. Thus the assumption of a monolith body for the calculation of the external stability is justified.

### 5.5 *Creep behaviour of the geogrid*

Although most of the deformation occurs after construction completion, the overall deformation behaviour is time dependent. In the regions of maximum extension of geogrids, the creep behaviour of the geogrid is shown in Figure 4. A decreasing tendency in deformation rate can be observed. The last readings were made in the summer of 2005 (observation period of 8 years). If the creep extensions e.g. of extensometer B are extrapolated to a service life of 120 years, chosen as the design life of the geogrid, an creep extension of 3.47% is obtained (compared to the strain at rupture of 15%). This clearly shows that there is still ample safety reserve, even though the preliminary design was carried out using design strength equal to the ultimate tensile strength of the geogrid.

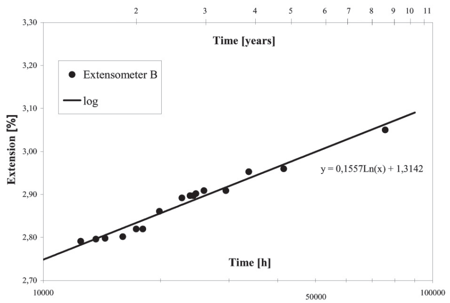


Figure 4. Creep behaviour of the geogrid in extensometer B.

### 5.6 *Determination of the critical failure surface*

During construction, all 3 extensometers show a rapid rise of extension in the front third of the testing slope. Towards the rear part, the extension declines in a fairly uniform manner as further layers are constructed. At the same time, the position of peak stress in geogrid shifts to slope interior.

Let us have a look at extensometer A and compare the location of maximum extension before and after the 6 top layers are placed on the 10 m high slope. Note that there is a berm of 1.5 m width between the 10 m slope and the top layers (see Figure 3). After the placement of the top layers, the location of the maximum extension along extensometer A shifts by about 1 m in the slope interior. It can be inferred that the potential failure surface also shifts to the slope interior by about 1 m. The measured location of the potential failure surface agrees well with the calculated potential failure surface by the method of local strength mobilization (Figure 5).

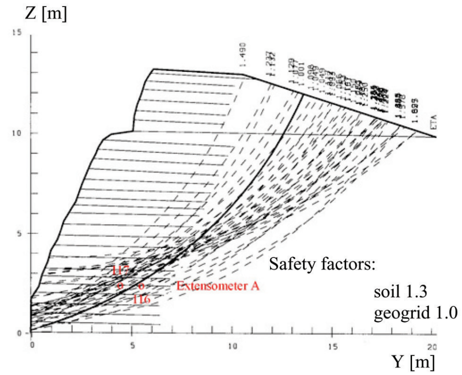


Figure 5. Critical failure surface.

## 6 CONCLUSION

Our investigation shows that the conventional design practice for reinforced slopes is too conservative. Even for a reduced embedment length of 6.5 m, the maximum stress and strain in the geogrid lie far below the corresponding design values. The interaction between geogrids and fill material plays should be taken into consideration to achieve economic design.

## ACKNOWLEDGEMENT


The project is financially supported by geotextile manufacturer Polyfelt Ltd based in Linz, Austria, the Austrian promotion agency and the landfill operator Ernst & Franz Kritsch Ltd in Vienna.


## REFERENCES


Bathurst, R.J., Blatz, J.A. and Burger, M.H. (2003) 'Performance of instrumented large-scale unreinforced and reinforced embankments loaded by a strip footing to failure', Can. Geotech. J. Vol. 40, 1067-1083.

Lai, T.Y., Ronaldo I. Borja, R.I., Duvernay, B.G. and Meehan, R.L. (2003), 'Capturing strain localization behind a geosynthetic-reinforced soil wall', Int. J. Numer. Anal. Meth. Geomech., Vol. 27, 425-451.

ÖNORM (Austrian Norm) B 4435-2 (1999) 'Shallow foundations – stability calculation based on Eurocode'